

Observation of surface states in a truncated two-dimensional photonic crystal slab

Yurii A. Vlasov,^{1,*} Nikolaj Moll,² and Sharee J. McNab¹

¹*IBM T. J. Watson Research Center, Yorktown Heights, NY 10598, USA*

²*IBM Research, Zurich Research Laboratory, Rüschlikon, Switzerland*

(Dated: November 20, 2018)

The effect of lattice termination on the surface states in a two-dimensional truncated photonic crystal slab is experimentally studied in a high index contrast silicon-on-insulator system. A single-mode silicon strip waveguide that is separated from the photonic crystal by a trench of variable width is used to evanescently couple to surface states in the surrounding lattice. It is demonstrated that the dispersion of the surface states depends strongly on the specific termination of the lattice.

Two-dimensional (2D) slab-type photonic crystals (PhC) are viewed as a promising platform for dense integration of discrete optical components into a photonic integrated circuit (PIC). In almost all of the optical devices based on 2D PhCs the periodicity of the PhC lattice is locally disrupted to give rise to localized states useful for the required functionality. However there is another general class of localized states in PhCs - surface states localized at the interface between the PhC and the surrounding media¹, which can become increasingly important for engineering dense PICs. As in any finite periodic system, the surface states in the PhC originate from the abrupt termination of the crystal's periodicity². Coupling of the waveguide modes or cavity resonances to surface states in improperly truncated PhC devices can disrupt light propagation and compromise device performance. Surface states can also affect the impedance, for example at the interface of a PhC waveguide and a strip waveguide³ and therefore different truncations of the lattice could be applied to improve impedance matching to reduce coupling losses. Beaming and focusing has also been recently demonstrated^{4,5} by changing the termination of the PhC lattice and hence surface states.

In this paper we present experimental studies of surface states in truncated 2D PhC slabs fabricated in silicon-on-insulator (SOI) wafers. 200mm diameter SOI wafers with 220nm thick silicon device layer on top of 2 μ m thick buried oxide (BOX) layer were patterned with electron beam lithography and processed on a standard CMOS fabrication line as reported elsewhere⁶. PhCs with a triangular lattice were defined by etching a periodic array of circular holes down to the BOX layer. The hole diameter D was set to 306nm with a lattice constant a of 437nm and a silicon slab thickness of $0.5a$ (220nm). Double-trench (DT) PhC waveguides consisting of a conventional strip waveguide embedded in a PhC lattice [7, 8], were explored as a model system for probing surface states. The core of the waveguide is formed by omitting one row of holes in the PhC lattice in the Γ - M direction and etching two parallel trenches to define the strip waveguide in the center. The width of the strip waveguide W embedded in the PhC slab was chosen to be $0.6a$ (263nm). The double-trench design of the PhC wave-

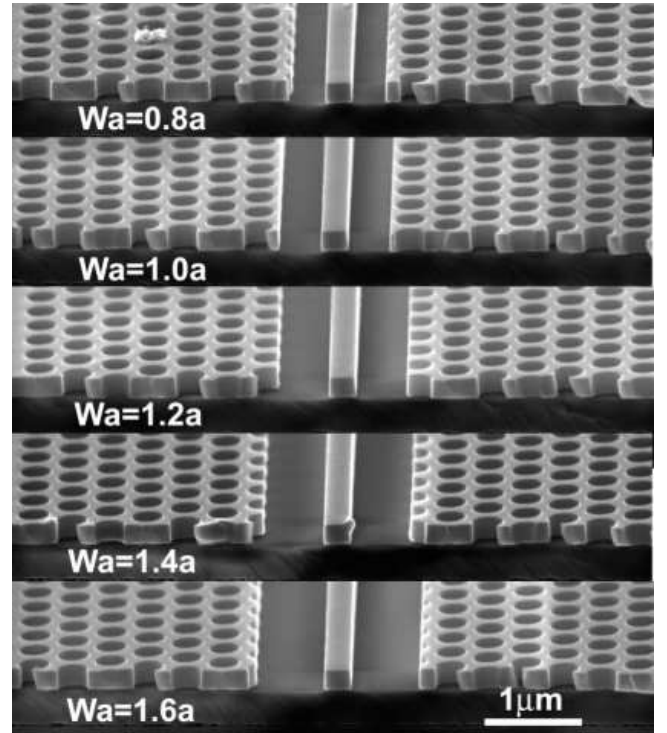


FIG. 1: Set of SEM images of the PhC DT waveguides with different trench width (W_a) varying from $0.8a$ to $1.6a$ (top to bottom).

uide allows the coupling between the modes in the strip and in the PhC to be varied by changing the width of the trench W_a that separates the strip from the surrounding PhC lattice. At the same time a different W_a implies a different truncation of the nearby holes of the PhC lattice as shown in Fig. 1, thus providing a tool to manipulate surface states.

Surface states are optically probed by inspecting the transmission through the DT PhC waveguide with different truncations of the PhC lattice adjacent to the waveguide channel. A pair of strip access waveguides of the same width W is used for coupling into and out of the

PhC waveguide. These narrow strip waveguides are adiabatically tapered to a wider access waveguide with a final width of 465nm. For efficient coupling of light into and out of the device-under-test (DUT) the access strip waveguides were terminated by a pair of spot-size converters based on an inverted taper design⁶. The light from a broadband (1200-1700nm) LED source is coupled to the DUT via a tapered and microlensed PM fiber and, after transmission through the DUT, is collected by a microlensed SM fiber and analyzed with an OSA. Further details of the experimental set-up are reported elsewhere⁶.

Transmission spectra for the TE polarization measured on a series of devices are shown in Fig. 2 for different trench widths W_a . The spectrum for the trench width of $W_a=1.6a$ can be used as a reference since the interaction with the PhC modes is negligible for such a wide trench and the spectrum is almost identical to that of the isolated strip waveguide. The spectrum is characterized by a nearly flat band transmission over a broad range of frequencies with a long-wavelength cut-off around $0.304c/a$ (wavelength of 1440nm). With the decrease of the trench width, and correspondingly the distance to the PhC, a narrow dip appears at $0.317c/a$ (wavelength of 1385nm). This dip was previously identified as originating from a narrow stopband appearing at the Brillouin-zone boundary⁸. The attenuation at the center of this dip gradually increases from 2.5dB to 26dB as the trench width is decreased from $1.4a$ to $0.8a$, and can be used as a measure of the magnitude of interaction of the mode in the strip waveguide with the periodic PhC lattice.

The spectrum for the trench width of $1.2a$ is drastically different from all other spectra in the set. Two new sharp bands with strong attenuation (over 18dB) appear at frequencies $0.322c/a$ and $0.325c/a$. According to theoretical predictions in Ref.7, the surface termination, which corresponds to $W_a = 1.2a$, is favorable for moving the surface states to the center of the photonic gap. Correspondingly these changes in the transmission spectrum can be interpreted as coupling of the mode in the strip waveguide to the surface states localized at the PhC interface. This interpretation is also supported by the analysis of the field pattern of the waveguiding mode shown in the inset of Fig. 2. The field pattern of the propagating mode was acquired with an IR camera through a 40X objective at the exit of a cleaved 500 μ m long DT PhC waveguide. The resulting image is a wavelength averaged field distribution in the waveguide as the source is a broadband LED. Examination of the field pattern reveals the dramatic change from a nearly Gaussian mode confined predominantly in the slab center for the properly terminated waveguide ($W_a=0.8a$) to a broadened mode that is delocalized over the whole slab owing to the excitation of surface states when $W_a=1.2a$.

To further analyze the interaction of the waveguiding mode with surface states, photonic band structures were calculated⁹. Different trench widths W_a and hence dif-

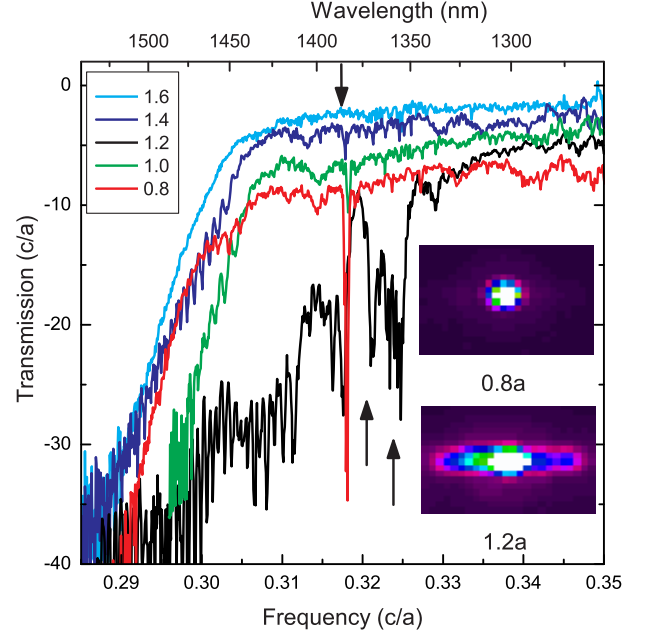


FIG. 2: Set of transmission spectra for TE-polarized light through DT PhC waveguides with different trench widths. Spectra were measured with a resolution of 0.5nm on waveguides 500 μ m long. The cyan, blue, black, green and red spectra correspond to nominal trench widths of $1.6a$, $1.4a$, $1.2a$, $1.0a$, and $0.8a$ respectively. Spectra are shifted vertically with respect to each other by 1dB for clarity. Inset: Field profiles of the TE-mode in DT PhC waveguides with trench widths of $0.8a$ (top) and $1.2a$ (bottom). The width of the field of view corresponds to 20 μ m.

ferent termination of the PhC surface are examined. As a reference the dispersion of the waveguiding mode for trench width of $1.6a$ is shown in Fig. 3b by a dashed black line. It is almost identical to the dispersion of the corresponding isolated strip waveguide, which is close to linear for most of the frequency range of interest. The sharp cut-off seen around 1440nm in the spectrum for the $W_a = 1.6a$ (green line in Fig. 3a), is consistent with the mode crossing the light line set by the silica cladding at $0.304c/a$.

The photonic band diagram for the PhC with the trench width $W_a=1.2a$ is shown by the magenta open circles in Fig. reffig3b. It is almost identical to the previous case except for the appearance of two surface modes which cross the fundamental mode at $0.327c/a$. For comparison with the band diagrams the experimental transmission spectra are presented in Fig. 3a for $W_a=1.6a$, $W_a=1.0a$ and two nominally designed $W_a=1.2a$ but fabricated with different exposure conditions. The origin of the sharp dips in the experimental spectra can be associated with the crossing of the surface modes with the guiding mode in the photonic band diagram. The sharp dip in the experimental spectrum for $W_a=1.2a$ (shown by

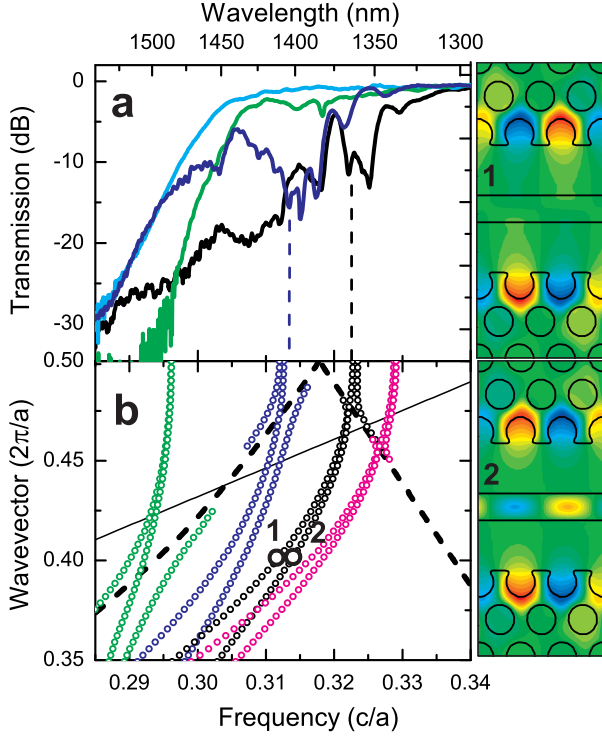


FIG. 3: (a): Set of transmission spectra for TE-polarized light for DT PhC waveguides with different widths of the trench. Spectra were measured with low resolution (5nm) on waveguides 500 μ m long. The cyan, green, blue and black spectra correspond to the samples with the trench width 1.6a, 1.0a, and two different nominally 1.2a, respectively. (b) Set of photonic band structures calculated for the TE-like modes for the DT PhC waveguides with different trench widths. Green, blue, black, and magenta open circles shows dispersion of only the surface modes for the trench width of 1.0a, 1.12a, 1.17a, and 1.2a, respectively. The dashed black curve represents the undisturbed dispersion of the PhC waveguide when surface states are pushed out of the photonic gap ($W_a=0.8a$). The thin solid black line represents the light line of the silica cladding layer. Right hand panel: In-plane magnetic field profiles of the two surface-localized modes calculated for $W_a=1.12a$ for the reduced wavevector of 0.4 (numbered 1 and 2 and marked in the main figure by open black circles).

a black line in Fig. 3a appears at $0.323c/a$, a frequency slightly lower than the crossing point of $0.327c/a$ seen in the band diagram. This roughly 3% difference could reasonably be attributed to a 3% error in determination of the lattice parameters of the experimental structure. Indeed if a slightly smaller trench width of $W_a=1.17a$ is assumed the photonic band calculations show a crossing at $0.323c/a$ (black open circles in Fig. 3b). The sharp dips around 1400nm in the blue spectrum in Fig. 3a (also a nominally $W_a=1.2a$ device but with a lower exposure dose) can be fitted in an analogous way by the band diagram for a trench width $W_a=1.12a$ (blue open circles in Fig. 3b). The transmission spectrum for a PhC with a

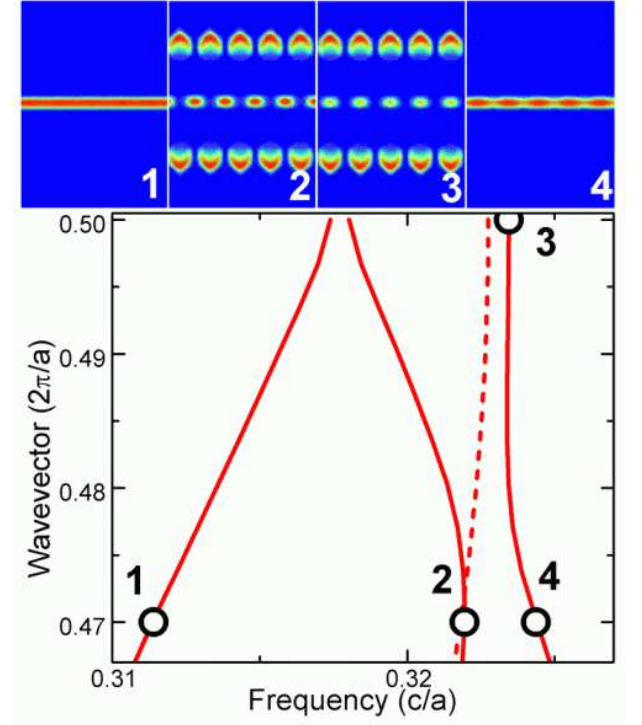


FIG. 4: Magnified view of the photonic band diagram for the TE-like modes for the DT PhC waveguides with the trench width of 1.17a. Solid (dashed) lines correspond to bands of even (odd) symmetry with respect to the xz plane bisecting the slab along the waveguide direction. Images 1-4 represent the in-plane time-averaged magnetic field power density calculated for corresponding wavevectors marked 1-4 in the photonic band diagram.

nominal trench width of $W_a=1.0a$ (green line in Fig. 3a does not differ considerably from the reference spectrum for $W_a=1.6a$ (cyan line in Fig. 3a). However close inspection reveals enhanced attenuation at frequencies below the light line cut-off, where bands associated with surface states cross the fundamental mode at around $0.295c/a$.

Further insight into the coupling to surface states can be provided by inspection of the magnetic field profiles. The right hand panel of Fig. 3 represents field profiles for the case of $W_a=1.17a$ calculated for the reduced wavevector of 0.4 far from the crossing region. Two surface modes form a pair of even and odd states with respect to the xz plane bisecting the slab along the waveguide direction. The odd mode (point 1) can not be excited from the input access strip waveguide and, correspondingly, it crosses the strip-localized fundamental mode without interaction and does not contribute to transmission. The even mode (point 2) has the same symmetry as the fundamental mode in the strip and, correspondingly, they can interact with each other at the crossing. This interaction can be further facilitated by the considerable field intensity of the even surface mode in the central strip waveguide.

Figure 4, a magnified portion of the band diagram for $W_a=1.17a$ around $0.323c/a$, reveals classical anti-crossing behavior. The time-averaged magnetic field energy density profiles for the fundamental mode related to the strip waveguide and the even surface mode are presented on top of Fig. 4. It is seen that for frequencies far away from the anti-crossing region (point 1) the field profile is localized predominantly in the central strip. At the anti-crossing of the strip-related mode and even surface mode two mixed states are formed: one which is mostly surface localized (point 2) and another mostly strip-localized (point 4). A mini-stopband forms at the anti-crossing resulting in strong attenuation of the transmission spectrum.

The transmission dip has a pronounced doublet structure indicating a more complex interaction. It can be suggested that the spectral shape of the transmission spectrum in the anti-crossing region is strongly affected by the efficiency of coupling from the access strip waveguide to the DT PhC waveguide. It is seen that the edges of the mini-stopband are formed by two states (points 2 and

3 in Fig. 4), which are predominantly surface-localized, and, correspondingly, have poor coupling efficiency to the access strip waveguides. Therefore attenuation can occur even for frequencies beyond the boundaries of the mini-stopband, with the spectral shape dependent on the way in which the energy in the mode is redistributed between states predominantly localized in the strip and the surface.

In conclusion, the influence of surface termination on the dispersion of surface states in truncated PhCs is experimentally demonstrated in a DT PhC waveguide system. Using photonic band calculations it is shown that sharp dips in the transmission spectra originate from coupling to surface modes. It is demonstrated that depending on the exact location of the truncation with respect to the unit cell of the PhC lattice the surface states can either be positioned at the center of the photonic gap where they interact strongly with the waveguiding mode in the strip waveguide, or be pushed away from the gap and do not contribute to transmission.

* Corresponding author; e-mail: yvlasov@us.ibm.com

- ¹ W. M. Robertson, G. Arjavalingam, R. D. Meade, K. D. Brommer, A. M. Rappe, and J. D. Joannopoulos, "Observation of surface photons on periodic dielectric arrays", *Opt. Lett.* **18**, 528 (1993).
- ² D. Kossel, "Analogies between thin-film optics and electron band theory of solids", *J. Opt. Soc. Am.* **56**, 1434 (1966).
- ³ J. Ushida et al., "Impedance matching for multidimensional open-system photonic crystals", *Phys. Rev. B* **68**, 155115 (2003)
- ⁴ E. Moreno, F. J. Garcia-Vidal, and L. Martin-Moreno, "Enhanced transmission and beaming of light via photonic crystal surface modes" *Phys. Rev. B*, **69**, 121402 (R) (2004).
- ⁵ P. Kramper et al., "Highly directional emission from photonic crystal waveguides of subwavelength width", *Phys.*

Rev. Lett. **92**, 113903 (2004).

- ⁶ S. J. McNab, N. Moll, and Yu. A. Vlasov, "Ultra-low loss photonic integrated circuit with membrane-type photonic crystal waveguides", *Optics Express*, **11**, 2927, 2003.
- ⁷ W. T. Lau, and S. Fan, "Creating large bandwidth line defects by embedding dielectric waveguides into photonic crystal slabs," *Appl. Phys. Lett.* **81**, 3915, 2002.
- ⁸ Yu. A. Vlasov, N. Moll and S. J. McNab, "Mode mixing in asymmetric double-trench photonic crystal waveguides", *Journ. Appl. Phys.*, **95**, 4095 (2004).
- ⁹ S. G. Johnson and J. D. Joannopoulos, "Block-iterative frequency-domain methods for Maxwell's equations in a planewave basis," *Optics Express* **8**, 173, 2001.